Radiotherapy and Oncology 141 (2019) 239–246

Contents lists available at ScienceDirect

Radiotherapy and Oncology

journal homepage: www.thegreenjournal.com

Original Article

Radiomic signature: A novel magnetic resonance imaging-based prognostic biomarker in patients with skull base chordoma

Wei Wei [a,b,c,h,1], Ke Wang [d,e,1], Zhenyu Liu [c,g,1], Kaibing Tian [d,e], Liang Wang [d,e], Jiang Du [f], Junpeng Ma [d,e], Shuo Wang [c,h], Longfei Li [c], Rui Zhao [a,b], Luo Cui [a,b], Zhen Wu [d,e,*], Jie Tian [b,c,g,h,*]

[a] School of Electronics and Information, Xi'an Polytechnic University; [b] Engineering Research Center of Molecular and Neuro Imaging of Ministry of Education, School of Life Science and Technology, Xidian University, Xi'an; [c] CAS Key Laboratory of Molecular Imaging, Institute of Automation, Chinese Academy of Sciences, Beijing; [d] Department of Neurosurgery, Beijing Tiantan Hospital, Capital Medical University; [e] China National Clinical Research Center for Neurological Diseases; [f] Department of Neuropathology, Beijing Neurosurgical Institute; [g] School of Artificial Intelligence, University of Chinese Academy of Sciences; and [h] Beijing Advanced Innovation Center for Big Data-Based Precision Medicine, School of Medicine, Beihang University, Beijing, China

ARTICLE INFO

Article history:
Received 29 March 2019
Received in revised form 12 August 2019
Accepted 1 October 2019
Available online 25 October 2019

Keywords:
Biomarkers
Magnetic resonance imaging
Prognosis
Progression-free survival
Radiomics
Skull base chordoma

ABSTRACT

Background and purpose: We used radiomic analysis to establish a radiomic signature based on anatomical magnetic resonance imaging (MRI) sequences and explore its effectiveness as a novel prognostic biomarker for skull base chordoma (SBC).

Materials and methods: In this retrospective study, radiomic analysis was performed using preoperative axial T_1 FLAIR, T_2-weighted, and enhanced T_1 FLAIR from a single hospital. The primary clinical endpoint was progression-free survival. A total of 1860 3-D radiomic features were extracted from manually segmented region of interest. Pearson correlation coefficient was used for feature dimensional reduction and a ridge regression-based Cox proportional hazards model was used to determine a radiomic signature. Afterwards, radiomic signature and nine other potential prognostic factors, including age, gender, histological subtype, dural invasion, blood supply, adjuvant radiotherapy, extent of resection, preoperative KPS, and postoperative KPS were analyzed to build a radiomic nomogram and a clinical model. Finally, we compared the nomogram with each prognostic factor/model by DeLong's test.

Results: A total of 148 SBC patients were enrolled, including 64 with disease progression. The median follow-up time was 52 months (range 4–122 months). The Harrell's concordance index of the radiomic signature was 0.745 (95% CI, 0.709–0.781) for the validation cohort, and its discrimination accuracy in predicting progression risk at 5 years in the same cohort was 82.4% (95% CI, 72.6–89.7%).

Conclusions: The radiomics is a low-cost, non-invasive method to predict SBC prognosis preoperatively. Radiomic signature is a potential prognostic biomarker that may allow the individualized evaluation of patients with SBC.

 Radiotherapy and Oncology 141 (2019) 239–246

Chordoma is a rare primary malignant bone tumor with an incidence of 1 every million individuals per year [1], and skull base chordomas (SBC) represent thirty percent of the cases [2]. SBC has poor prognosis and a 10-year survival rate of 58.7% [3]. The poor outcome is primarily due to a high rate of local recurrence [4], which was reported to be as high as 68% [5], with most recurrences occurring within 5 years after the initial surgery [6]. Local recurrence of SBC is the marker of treatment failure, and novel prognostic biomarkers are urgently needed [7]. Current studies indicate that gender is associated with SBC prognosis [8], while the pathologic and perioperative Karnofsky performance status (KPS) are also potential prognostic biomarkers [6], as are the extent of tumor removal and postoperative radiation therapy [9]. However, because of the rarity of the disease, the number of case samples reported in these studies is usually small, so that these potential SBC prognostic factors are still controversial [10].

Abbreviations: MRI, magnetic resonance imaging; SBC, skull base chordoma; PFS, progression-free survival; FLAIR, fluid attenuated inversion recovery; PACS, picture archiving and communication system; DICOM, digital imaging and communications in medicine; KPS, karnofsky performance status; CI, confidence interval; AUC, area under curves; ROI, region of interest.

* Corresponding authors at: Department of Neurosurgery, Beijing Tiantan Hospital, Capital Medical University, 119 West Road of South Fourth Ring, Fengtai District, Beijing 100050, China (Z. Wu). CAS Key Laboratory of Molecular Imaging, Institute of Automation, Chinese Academy of Sciences, Beijing, 100190, China (J. Tian).

E-mail addresses: wuzhen1966@aliyun.com (Z. Wu), jie.tian@ia.ac.cn (J. Tian).

[1] Wei Wei, Ke Wang, and Zhenyu Liu contributed equally to this work.

https://doi.org/10.1016/j.radonc.2019.10.002
0167-8140/

Magnetic resonance imaging (MRI), a routinely used diagnostic tool [11], provides a non-invasive and low-cost method for extracting prognostic information in SBC [12,13]. Radiomics [14], a subset of the field of medical imaging research based on the technology of machine learning, has progressed dramatically in recent years, enabling a comprehensive expression of tumor heterogeneity and more advanced prognostic applications [15]. Establish a prognostic model using high-throughput quantitative radiomic features extracted from medical images provides a novel potential tool for clinicians to implement personalized treatment plans and prognosis assessments [16–19]. Furthermore, our previous radiomic analyses have been successfully applied in many different oncological diseases [20–25] and clarified the relationship between radiomic features and prognosis [26,27]. Therefore, radiomics may also provide a potential tool for analyzing the prognosis of SBC [28–32].

In this retrospective study, we hypothesized that radiomic analysis would provide a prognostic biomarker for SBC in the form of a radiomic signature. We performed radiomic analysis to extract MRI-based quantitative radiomic features and developed a novel radiomic signature for individualized, pretreatment evaluation of progression-free survival (PFS) in patients with SBC. Collectively, these findings provide potentially critical insights for individualized treatment and follow-up planning.

Materials and methods

We enrolled 148 patients with SBC, between January 2005 and July 2014, at the Beijing Tiantan Hospital, Capital Medical University. The ethics committee of the Hospital approved this study and informed consent was obtained from all participants. Our study was conducted in accordance with the Declaration of Helsinki, TRIPOD, and Guidelines of Luo et al [33,34]. The study design is illustrated in Fig. 1.

Eligibility criteria

Patient inclusion criteria were: (a) pathologically confirmed SBC, (b) diagnosis made and surgery performed at our hospital, and (c) preoperative MRI images stored in the Picture Archiving and Communication System (PACS), including axial T_1 FLAIR, axial T_2-weighted, and enhanced axial T_1 FLAIR sequences. Patient exclusion criteria were: (a) patients without a history of tumor resection, (b) patients without follow-up data, and (c) incomplete clinical information or MRI sequences.

We retrospectively reviewed the inpatient records of enrolled patients and collected potential prognostic factors that might be associated with the prognosis of SBC, including age [10], gender [8], histological subtypes [6], dural invasion [4], blood supply [35], extent of resection [4], adjuvant radiotherapy [9], preoperative KPS, and postoperative KPS [6].

The enrolled patients were divided into a training cohort and a validation cohort based on the time of surgery: patients who underwent surgery between January 2005 and December 2009 formed the training cohort, and patients who underwent surgery between January 2010 and July 2014 formed the validation cohort. In addition, the enrolled patients were re-divided into another training cohort and another validation cohort by random number at a 1:2 ratio. The details of primary treatment have been described in our previous studies [4,6]. Details of study inclusion and exclusion criteria (Fig. A.1), follow-up, clinical endpoints, MRI technique, and tumor segmentation are described in the Appendix.

Radiomic feature extraction and radiomic signature building

The DICOM images and segmentation matrices were normalized according to pixel spacing. Radiomic features expressing tumor characteristics were high-dimensional quantitative features extracted from the region of interest (ROI) of the MRI images. Based on our radiomics platform (www.radiomics.net.cn) and our previous research [23,24,32], we extracted 620 3-D radiomic features from each MRI sequence (for a total of 1860 features, Table A.1) [36]. Details of radiomic feature extraction are described in the Appendix.

Due to the high dimensional nature of the radiomic features extracted, over-fitting would have occurred if all 1860 radiomic features were used to build a radiomic signature. Therefore, we used Pearson correlation coefficient to select the features that were most associated with prognosis in the training cohort with a cut-off value of $P < 0.05$. And then tested the inter-correlation between the features of $P < 0.05$ to minimize number of the features. The

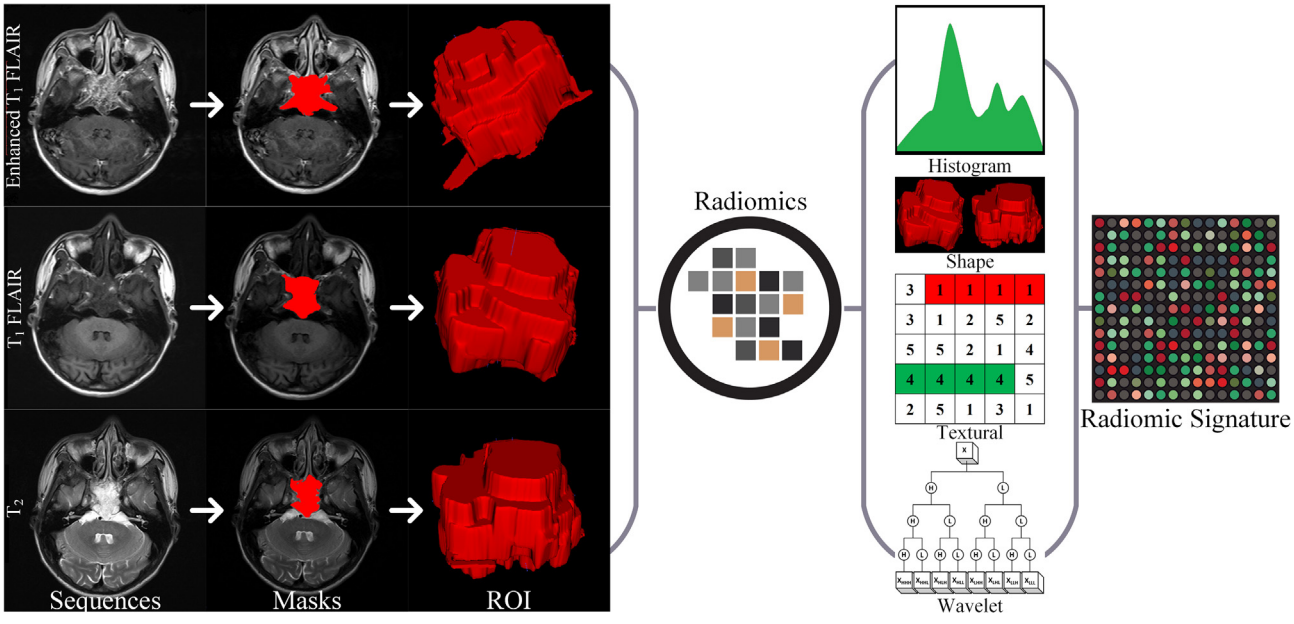

Fig. 1. Study flowchart. The flowchart of our study. The three MRI sequences in the figure are from the same location of a same patient. ROI, region of interest.

cut-off value was defined as the absolute value of correlation coefficient >0.8. A ridge regression-based Cox proportional hazards model was used to test the relationship between these features and PFS [37]. The ridge regression coefficients of the selected features were used to develop a novel prognostic biomarker (namely, a radiomic signature) for predicting the individual risk of disease progression. The radiomic signature score for each patient was a linearly-weighted combination of the selected features.

In order to facilitate clinical application, we normalized the radiomic signature according to Eq. (1), thus transforming it into a continuous risk score ranging between 0 and 1, with higher scores indicating a greater probability of poor prognosis. The radiomic signature was further stratified into low and high risk via the x-tile [38] and recursive partitioning analysis (RPA) [39], respectively. Radiomic feature extraction, dimensional reduction, and radiomic signature construction were implemented using MATLAB R2016a (MathWorks, Natick, MA).

$$Normalized\ signature = \frac{Signature - Training_{min}}{Training_{max} - Training_{min}} \quad (1)$$

Prognostic factors validation

The potential association between prognostic factors (including radiomic signature) and PFS was validated in the validation cohort. Kaplan-Meier survival analysis and log-rank test were used to determine the relationship between the categorical radiomic signature and PFS, as well as the nine other potential prognostic factors. The cut-off value of age was calculated using the Youden index [40].

Furthermore, a univariate Cox proportional hazards model was used to calculate the Harrell's concordance index (C-index) for the continuous radiomic signature and nine other potential prognostic factors. A multivariate regression analysis was performed using Akaike Information Criterion [41] (AIC) for factors with a result of $P < 0.05$ in univariate Cox regression analysis. Multivariable Cox proportional hazards models were built for developing a radiomic prognosis nomogram [42] (including continuous radiomic signature) and a clinical prognosis model (excluding continuous radiomic signature) using the factors selected by AIC. Afterwards, we used the continuous radiomic signature, nine other potential prognostic factors, radiomic prognosis nomogram, and clinical prognosis model to predict the individual probabilities of 5-year PFS after surgery. Radiomic signature and age were used as continuous variables, while the other eight factors were used as categorical variables. These prognostic models were used to predict the individual probabilities of 5-year PFS and the discriminant accuracy of the Cox models were evaluated using the time-dependent area under curves (AUC) [43]. The DeLong's test was used to compare the radiomic prognosis nomogram and each clinical factor/-model [44].

The 95% confidence interval (CI) of the C-indices and AUCs were calculated by bootstrapping with 1000 resampling. The calibration curves were used to assess the degree of variability of the predictions and to compare the PFS with the true PFS in the validation cohorts [45]. The calibration curves were tested using the Hosmer-Lemeshow test to determine whether the predicted curve and the true curve significantly differed [46].

Statistical analysis

Median and range were reported for age and follow-up time, whereas frequencies and proportions were reported for categorical variables including the categorical radiomic signature. Differences in continuous variables and categorical variables were assessed using the independent samples t-test and Fisher exact test, respectively. All statistical tests were two-sided. Significance was set as $P < 0.05$. Validation of the prognostic factors and statistical analysis were implemented with R version 3.6.1 (R Foundation for Statistical Computing, Vienna, Austria).

Results

Overall, 148 patients were enrolled. Fifty patients formed the training cohort, and 98 patients formed the validation cohort. The primary demographic and clinical data of the training and validation cohorts are listed in Table A.2 and Table 1, respectively. The data of training cohort are described in the Appendix. In the validation cohort, thirty-eight (39%) patients had documented progression during the follow-up. The median (range) PFS was 17.5 months (4–67 months) in the progression patients, and the median (range) follow-up time was 52 months (4–122 months) in the censored patients. There were no statistically significant differences between the progression and no progression groups in potential prognostic variables with the exception of categorical radiomic signature ($P < 0.001$) and histological subtype ($P = 0.006$). There were 57 (58%) conventional SBC patients, and these patients had significantly poor prognoses. There were no dedifferentiated SBC enrolled in our study. Radiomic signature and histological subtype had significant statistical differences between the progression group and no progression group in the training and validation cohorts. All experimental results of the randomly divided samples are described in the Appendix (Table A.5, Fig. A.5, Fig. A.6).

We calculated the ICC of the radiomic features using the ROI selected by the two radiologists. The ICC values (range, 0.89–0.98) showed that the features were stable between two radiologists. Based on the training cohort, we selected, among the 1,860 high-dimensional radiomic features, the fifteen features that were most strongly associated with PFS to build a radiomic signature. The details of the selected radiomic features are described in Table A.3.

The radiomic signature was an effective prognostic biomarker when used as a categorical variable. Low risk was defined as radiomic signature score <0.5 and high risk as score ≥0.5 via the x-tile. Statistically significant discrimination of the PFS among the high-risk and low-risk progression groups, divided by the categorical radiomic signature, was observed in the training and validation cohorts (Fig. 2). Both *p*-values of log-rank test were <0.001. In the validation cohort, there were 63 (64%) patients in the high-risk group, including 36 (57%) patients with progression (Table 2), while there were 35 (36%) patients in the low-risk group, including 2 (6%) patients with progression. The low-risk group thus had a significantly better prognosis than high-risk group ($P < 0.001$). The categorical radiomic signature showed a high sensitivity of 94.7% and a low false negative rate of 5.3%. Meanwhile, the accuracy and specificity were 70.4% and 55.0%, respectively. There were no statistical differences between the groups in the follow-up time of censored patients ($P = 0.758$). Among the nine other potential clinical prognostic factors, histological subtype ($P = 0.002$) and blood supply ($P = 0.031$) of the tumor were statistically different PFS between their subgroups (Fig. A.4, Table A.4). The performance of RPA-based categorical radiomic signature are described in the Appendix (Fig. A.2 and Fig. A.3).

In the univariate Cox analyses, the C-index of the continuous radiomic signature was 0.745 (95% CI, 0.709–0.781) in the validation cohort (Table A.4). The discrimination accuracy of the continuous radiomic signature for predicting 5-year progression risk was 82.4% (95% CI, 72.6%-89.7%) in the same cohort (Fig. 3A, Table A.4). The Cox model of the continuous radiomic signature also demonstrated favorable calibration in the validation cohort (Fig. 3B).

Table 1
Descriptive statistics of patients with chordoma in validation cohort.

Variable	Validation (N = 98)	Progression (n = 38)	No progression (n = 60)	*P*
Age at surgery (years), median (range)	38 (5–67)	38 (11–58)	38 (5–67)	0.977
Gender (%)				0.673
Male	58 (59)	24 (63)	34 (57)	
Female	40 (41)	14 (37)	26 (43)	
Histological subtypes (%)				0.006
Conventional	57 (58)	29 (76)	28 (47)	
Chondroid	41 (42)	9 (24)	32 (53)	
Dedifferentiated	0 (0)	0 (0)	0 (0)	
Dural invasion (%)				1.000
Intradural	34 (35)	13 (34)	21 (35)	
Extradural	64 (65)	25 (66)	39 (65)	
Blood supply (%)				0.096
Abundant	53 (54)	25 (66)	28 (47)	
Poor	45 (46)	13 (34)	32 (53)	
Extent of resection (%)				0.404
<70%	3 (3)	0 (0)	3 (5)	
70–90%	15 (15)	8 (21)	7 (12)	
90–100%	63 (64)	24 (63)	39 (65)	
100%	17 (17)	6 (16)	11 (18)	
Adjuvant radiotherapy (%)				0.290
Yes	39 (40)	18 (47)	21 (35)	
No	59 (60)	20 (53)	39 (65)	
Preoperative KPS (%)				0.116
≤60	9 (9)	6 (16)	3 (5)	
70	17 (17)	6 (16)	11 (18)	
80	42 (43)	19 (50)	23 (38)	
90	29 (30)	7 (18)	22 (37)	
100	1 (1)	0 (0)	1 (2)	
Postoperative KPS (%)				0.629
≤60	12 (12)	7 (18)	5 (8)	
70	9 (9)	4 (11)	5 (8)	
80	30 (31)	11 (29)	19 (32)	
90	44 (45)	15 (39)	29 (48)	
100	3 (3)	1 (3)	2 (3)	
Radiomics signature (%)				<0.001
High risk	63 (64)	36 (95)	27 (45)	
Low risk	35 (36)	2 (5)	33 (55)	
Follow-up time (months), median (range)	42 (4–122)	17.5 (4–67)	52 (4–122)	–

p-values are the result of Fisher exact tests (categorical variables) or independent-samples t-tests (continuous variables).
Abbreviations: KPS, Karnofsky performance status.

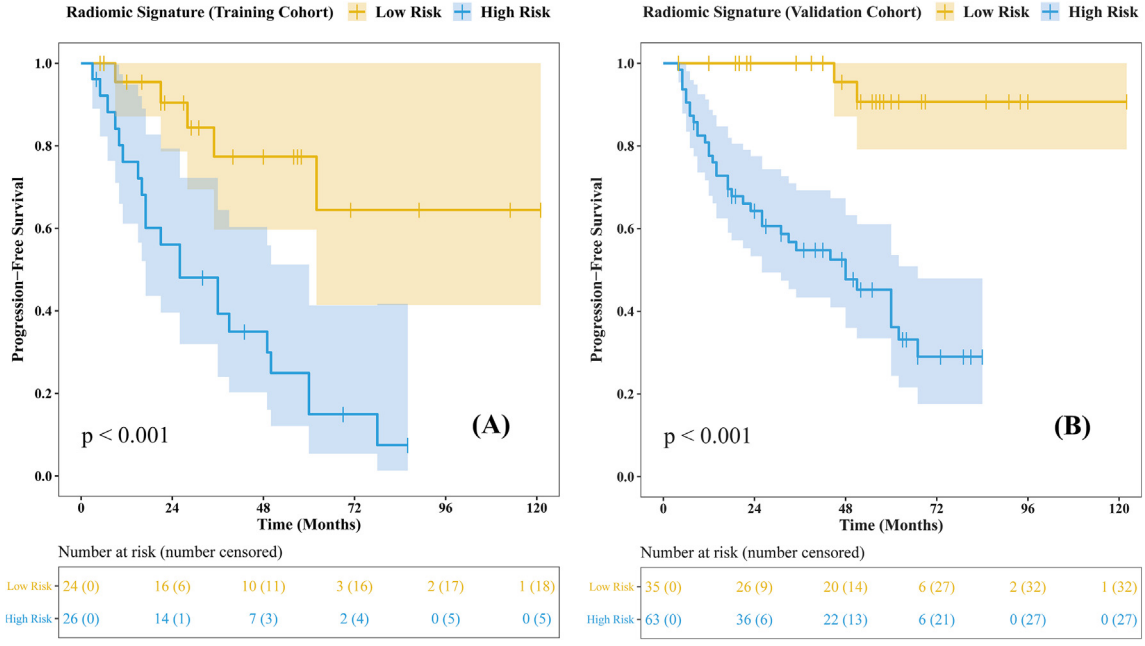

Fig. 2. Progression-free survival stratified by risk according to categorical radiomic signature. Kaplan-Meier curves showing progression-free survival in patients stratified by categorical radiomic signature and classification in the training (A) and validation (B) cohorts. High-risk and low-risk curves are compared with the log-rank test.

Table 2
Descriptive statistics of patients with chordoma in high/low risk groups of validation cohort.

Variable	High risk (n = 63)	Low risk (n = 35)	*P*
Age at surgery (years), median (range)	39 (11–67)	36 (5–63)	0.064
Gender (%)			0.523
Male	39 (62)	19 (54)	
Female	24 (38)	16 (46)	
Histological subtypes (%)			0.200
Conventional	40 (63)	17 (49)	
Chondroid	23 (37)	18 (51)	
Dedifferentiated	0 (0)	0 (0)	
Dural invasion (%)			0.507
Intradural	20 (32)	14 (40)	
Extradural	43 (68)	21 (60)	
Blood supply (%)			0.138
Abundant	38 (60)	15 (43)	
Poor	25 (40)	20 (57)	
Adjuvant radiotherapy (%)			
Yes	27 (43)	12 (34)	0.519
No	36 (57)	23 (66)	
Extent of resection (%)			0.362
<70%	1 (2)	2 (6)	
70–90%	12 (19)	3 (8)	
90–100%	40 (63)	23 (66)	
100%	10 (16)	7 (20)	
Preoperative KPS (%)			0.244
≤60	8 (13)	1 (3)	
70	13 (19)	4 (10)	
80	24 (40)	18 (55)	
90	17 (26)	12 (32)	
100	1 (2)	0 (0)	
Postoperative KPS (%)			0.068
≤60	11 (15)	1 (6)	
70	8 (13)	1 (3)	
80	17 (28)	13 (32)	
90	25 (40)	19 (55)	
100	2 (4)	1 (3)	
Progression (%)			<
Yes	36 (57)	2 (6)	0.001
No	27 (43)	33 (94)	
Follow-up time in censored patients (months), median (range)	50 (8–84)	55 (4–122)	0.758

p-Values are the result of Fisher exact tests (categorical variables) or independent-samples t-tests (continuous variables) for high-risk and low-risk groups. The high and low risk groups are divided by the radiomic signature score of each patient, the cut-off value is 0.5.
Abbreviations: KPS, Karnofsky performance status.

The *p*-value of the Hosmer-Lemeshow test for the 5-year PFS predictive ability of the continuous radiomic signature was 0.29. Among nine other potential clinical prognostic factors, only the histological subtype had a certain prognostic ability (C-index and time-dependent AUC > 0.6), but it still showed a significant difference (DeLong's test $P < 0.001$) compared with the radiomic prognosis nomogram (Fig. 4) in predictive performance (Fig. 3A, Table A.4). Moreover, continuous radiomic signature ($P < 0.001$), histological subtype ($P = 0.004$), and blood supply ($P = 0.035$) had statistical differences in the univariate Cox analyses, and the three factors had also been selected by AIC.

In the multivariable Cox analyses, the C-indices of clinical model and combined model (radiomic signature + clinical model, namely, radiomic prognosis nomogram, Fig. 4) were 0.684 (95% CI, 0.644–0.724) and 0.768 (95% CI, 0.734–0.803) in the validation cohort, respectively (Table A.4). And the discrimination accuracies for predicting 5-year progression risk were 73.0% (95% CI, 59.4%-80.2%) and 84.6% (95% CI, 74.2%-91.1%) in the same cohort, respectively (Fig. 3A, Table A.4). The combined model also demonstrated favorable calibration in the validation cohort (Fig. 3B). The *p*-value of the Hosmer-Lemeshow test was 0.34. The clinical model showed a significant difference (DeLong's test $P = 0.003$) compared with the radiomic prognosis nomogram in predictive performance (Fig. 3A, Table A.4).

Discussion

In the present retrospective study, we adopted a radiomic analysis using anatomical MRI images to develop a radiomic signature and a radiomic nomogram in a training cohort for SBC patients. Afterwards, we tested their prognostic utility for the validation cohort using Kaplan-Meier survival analysis, univariate and multivariate Cox regression analysis.

We confirm that histological subtype is a prognostic indicator in SBC, with chondroid SBC characterized by better prognosis [10]. Meanwhile, whether other factors can be identified as prognostic factors is controversial and remains to be further explored [5,6,8,9]. Although it is generally believed that the largest possible extent of the resection is a predictor of better prognosis, whether the extent of resection can be identified as a prognostic factor might depend on the surgical approach and the tumor location.

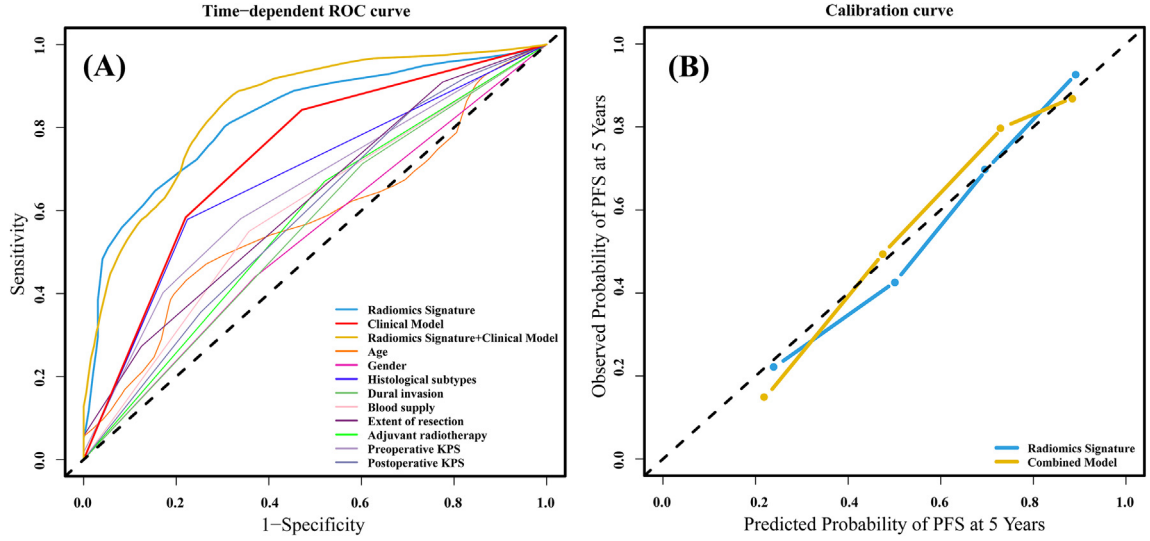

Fig. 3. Time-dependent ROC curves and calibration curves. Time-dependent ROC curves for the continuous radiomic signature, clinical prognosis model, radiomic prognosis nomogram, and nine other potential prognostic factors predicting 5-year PFS in the validation cohort (A). Calibration curves of 5-year time-dependent ROC curves of continuous radiomic signature and radiomic prognosis nomogram (B). The patients of validation cohort were divided into 4 groups for calibrations, each group containing at least 24 samples. ROC, receiver operating characteristic; PFS, progression-free survival.

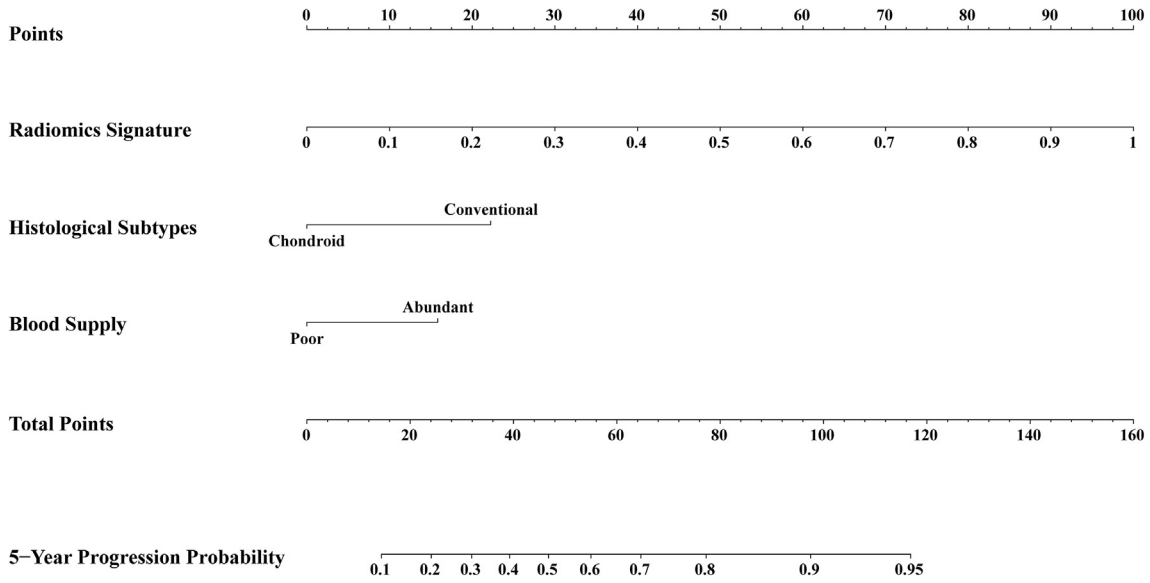

Fig. 4. Radiomic prognosis nomogram. Probability of 5-year progress-free survival in patients with skull base chordoma using the radiomic nomogram, which was developed by continuous radiomic signature, histological subtypes, and blood supply.

Some scholars argue that resection requires caution [5]. Moreover, whether to carry out postoperative adjuvant radiotherapy still needs further study [10]. The relative radioresistance of chordoma cells demands the administration of high-dose irradiation to sensitive regions, so that overtreatment and radiation toxicity are problems to be considered.

Radiomics has the capability to mine prognostic information from MRI [14,18,47]. In addition, radiomic analysis is feasible in preoperative, low-cost, and non-invasive prediction of prognosis based on MRI [19]. Due to the high heterogeneity among chordoma patients, predicting progression risk is challenging [48,49]. However, radiomic analysis is possible to provide an additional method by which tumor heterogeneity can be characterized [36]. Therefore, distinct radiomic signature might guide clinical practice together with other clinical factors such as histological subtype.

In the present study, we extracted a total of 1860 3-D radiomic features from three MRI sequences. Although the rapid development of deep learning algorithms produced a major breakthrough in the field of radiomics [50,51], it is not suitable for rare diseases such as chordoma, where the limited training samples risks making deep learning shallow, and discriminative features difficult to learn. And the radiomic features with interpretability were different from deep learning features, which were generally lacking interpretability. Therefore, radiomic analysis using hand-crafted features with specific explanations may be more suitable for this rare disease study [52]. Ridge regression is a biased estimation regression method suitable for collinear data analysis, which by abandoning the unbiasedness of the least squares method gains in realism and reliability of the regression coefficients, at the cost of losing part of the information and some accuracy [53]. We used this approach in the present study to prevent the fifteen selected radiomic features from overfitting.

Although the MRI images used in this study were acquired during nearly 10 years, we found little impact of this variability on the prognostic model's predictive validity, as verified in validation cohort. Rather than randomly dividing patients, we grouped patients by surgery time (early vs. late). This revealed that the model built on the training data, i.e. past patients, could be used to predict the prognoses of new patients. This design increased the generalization ability of the prognostic model.

The categorical radiomic signature stratified the validation cohort patients into high-risk and low-risk groups with significantly different PFS. The prediction results for 5-year PFS revealed that MRI-based radiomic analysis successfully stratified patients according to their continuous radiomic signature. Moreover, the performance of the radiomic signature and nomogram outperformed nine other prognostic factors and clinical model. Although common prognostic factors could be used to predict the prognosis of SBC [54–57], our experimental results indicate that their predictive ability is limited. Therefore, the use of the radiomics not only allows for the prediction of progression, but also complements existing SBC prognostic biomarkers.

There are few studies of MRI-based radiomic analysis of PFS in SBC. Yin et al [28–30] and Wei et al [31] have conducted radiomics-based chordoma research. Yin et al are the pioneers of radiomics in the application of chordoma. However, Yin's researches were the differential diagnosis of sacral chordoma, which did not involve the prognosis of chordoma. And the scan position of MRI/CT were different from our study. Wei's research could predict the recurrence probability of SBC. However, the use of a single T_2-weighted imaging sequence and a survival analysis method that did not enrolled censored data limited the generalization ability of their model. The present study not only validates previous research results on the value of radiomics in prognosis and confirms the value of radiomics in better understanding tumor prognosis, but also complements the prognostic biomarkers of SBC. Additionally, high risk SBC patients might be identified using this technique, so that more intensive treatments might be administered [5], and follow-up intervals might be shortened. This additional information might also affect the decision of using an adjuvant radiotherapy plan. High-risk patients might need strong recommendations for postoperative adjuvant radiotherapy, while low-risk patients might not receive adjuvant radiotherapy. Thus, this additional method of risk stratification in SBC patients might have a positive impact on improving treatment, avoiding overtreatment, and prolonging survival.

While the present study offers significant benefits, it also has some limitations which warrant discussion. First, because of the extremely low incidence of chordoma, it was a retrospective study with a relatively small sample size. A multicenter, prospective clinical trial is thus required to address the limitation. Additionally, manual segmentation was used, which may have resulted in inconsistent, subjective tumor segmentation, thereby reducing the model's performance. Based on our previous findings, further studies of

automatic segmentation algorithms are required to address this limitation [58].

In conclusion, radiomics may allow predicting SBC prognosis. These low-cost non-invasive methods, which can be used before surgery, are likely to affect the planning of clinical treatment and follow-up. Our results using the prognostic model suggest that the radiomic signature we developed is a prognostic biomarker of individual differences in SBC.

Conflict of interest

The authors declare that the research was conducted in the absence of any commercial or financial relationships that could be construed as a potential conflict of interest.

Acknowledgments

This work was supported by the National Natural Science Foundation of China [81922040, 81772012, 81227901, 81527805, 81672506, 81802683]; the National Key Research and Development Plan of China [2017YFA0205200, 2016YFA0100900, 2016YFA0100902]; the Beijing Natural Science Foundation [7182109]; the Beijing Natural Science Foundation [7182109]; the Youth Innovation Promotion Association CAS [2019136]; the Chinese Academy of Sciences [GJJSTD20170004, QYZDJ-SSW-JSC005]; and the Special Found for The Talents of Beijing [2016000021469G212]. The authors would like to acknowledge the instrumental and technical support of the multi-modal biomedical imaging experimental platform at the Chinese Academy of Sciences Institute of Automation.

Appendix A. Supplementary data

Supplementary data to this article can be found online at https://doi.org/10.1016/j.radonc.2019.10.002.

References

[1] McMaster ML, Goldstein AM, Bromley CM, Ishibe N, Parry DM. Chordoma: incidence and survival patterns in the United States, 1973–1995. Cancer Cause Control 2001;12:1–11.
[2] Stacchiotti S, Sommer J, Grp CGC. Building a global consensus approach to chordoma: a position paper from the medical and patient community. Lancet Oncol 2015;16:E71–83.
[3] Chambers KJ, Lin DT, Meier J, Remenschneider A, Herr M, Gray ST. Incidence and survival patterns of cranial chordoma in the United States. Laryngoscope 2014;124:1097–102.
[4] Wang L, Wu Z, Tian KB, Wang K, Li D, Ma JP, et al. Clinical features and surgical outcomes of patients with skull base chordoma: a retrospective analysis of 238 patients. J Neurosurg 2017;127:1257–67.
[5] Jian BJ, Bloch OG, Yang I, Han SJ, Aranda D, Tihan T, et al. Adjuvant radiation therapy and chondroid chordoma subtype are associated with a lower tumor recurrence rate of cranial chordoma. J Neuro-Oncol 2010;98:101–8.
[6] Tian KB, Zhang HY, Ma JP, Wang K, Ru XJ, Du J, et al. Factors for overall survival in patients with skull base chordoma: A retrospective analysis of 225 patients. World Neurosurg 2017;97:39–48.
[7] Walcott BP, Nahed BV, Mohyeldin A, Coumans JV, Kahle KT, Ferreira MJ. Chordoma: current concepts, management, and future directions. Lancet Oncol 2012;13:E69–76.
[8] Rachinger W, Eigenbrod S, Dutzmann S, Simon M, Feigl GC, Kremenevskaja N, et al. Male sex as a risk factor for the clinical course of skull base chordomas Clinical article. J Neurosurg 2014;120:1313–20.
[9] Boari N, Gagliardi F, Cavalli A, Gemma M, Ferrari L, Riva P, et al. Skull base chordomas: clinical outcome in a consecutive series of 45 patients with long-term follow-up and evaluation of clinical and biological prognostic factors. J Neurosurg 2016;125:450–60.
[10] Zou MX, Lv GH, Zhang QS, Wang SF, Li J, Wang XB. Prognostic factors in skull base chordoma: A systematic literature review and meta-analysis. World Neurosurg 2018;109:307–27.
[11] Liu ZY, Zhang YM, Yan H, Bai LJ, Dai RW, Wei WJ, et al. Altered topological patterns of brain networks in mild cognitive impairment and Alzheimer's disease: A resting-state fMRI study. Psychiat Res-Neuroim 2012;202:118–25.
[12] Lin E, Scognamiglio T, Zhao Y, Schwartz TH, Phillips CD. Prognostic Implications of Gadolinium Enhancement of Skull Base Chordomas. Am J Neuroradiol 2018;39:1509–14.
[13] Tian K, Wang L, Ma J, Wang K, Li D, Du J, et al. MR imaging grading system for skull base chordoma. Am J Neuroradiol 2017;38:1206–11.
[14] Lambin P, Rios-Velazquez E, Leijenaar R, Carvalho S, van Stiphout RGPM, Granton P, et al. Radiomics: Extracting more information from medical images using advanced feature analysis. Eur J Cancer 2012;48:441–6.
[15] Kumar V, Gu Y, Basu S, Berglund A, Eschrich SA, Schabath MB, et al. Radiomics: the process and the challenges. Magn Reson Imaging 2012;30:1234–48.
[16] Sun R, Limkin EJ, Vakalopoulou M, Dercle L, Champiat S, Han SR, et al. A radiomics approach to assess tumour-infiltrating CD8 cells and response to anti-PD-1 or anti-PD-L1 immunotherapy: an imaging biomarker, retrospective multicohort study. Lancet Oncol 2018;19:1180–91.
[17] Bae S, Choi YS, Ahn SS, Chang JH, Kang SG, Kim EH, et al. Radiomic MRI phenotyping of glioblastoma: improving survival preciction. Radiology 2018;289:797–806.
[18] Lambin P, Leijenaar RTH, Deist TM, Peerlings J, de Jong EEC, van Timmeren J, et al. Radiomics: the bridge between medical imaging and personalized medicine. Nat Rev Clin Oncol 2017;14:749–62.
[19] Aerts HJWL. The potential of radiomic-based phenotyping in precision medicine a review. JAMA Oncol 2016;2:1636–42.
[20] Wang S, Shi J, Ye Z, Dong D, Yu D, Zhou M, et al. Predicting EGFR mutation status in lung adenocarcinoma on CT image using deep learning. Eur Respir J 2019;53.
[21] Liu Z, Li Z, Qu J, Zhang R, Zhou X, Li L, et al. Radiomics of multi-parametric MRI for pretreatment prediction of pathological complete response to neoadjuvant chemotherapy in breast cancer: a multicenter study. Clin Cancer Res 2019.
[22] Liu ZY, Zhang XY, Shi YJ, Wang L, Zhu HT, Tang ZC, et al. Radiomics analysis for evaluation of pathological complete response to neoadjuvant chemoradiotherapy in locally advanced rectal cancer. Clin Cancer Res 2017;23:7253–62.
[23] Liu Z, Wang Y, Liu X, Du Y, Tang Z, Wang K, et al. Radiomics analysis allows for precise prediction of epilepsy in patients with low-grade gliomas. NeuroImage Clin 2018;19:271–8.
[24] Liu ZY, Wang S, Dong D, Wei JW, Fang C, Zhou XZ, et al. The applications of radiomics in precision diagnosis and treatment of oncology: opportunities and challenges. Theranostics 2019;9:1303–22.
[25] Xi YB, Guo F, Xu ZL, Li C, Wei W, Tian P, et al. Radiomics signature: A potential biomarker for the prediction of MGMT promoter methylation in glioblastoma. J Magn Reson Imaging 2018;47:1380–7.
[26] Wang S, Liu Z, Rong Y, Zhou B, Bai Y, Wei W, et al. Deep learning provides a new computed tomography-based prognostic biomarker for recurrence prediction in high-grade serous ovarian cancer. Radiother Oncol 2019;132:171–7.
[27] Wei W, Liu Z, Rong Y, Zhou B, Bai Y, Wei W, et al. A computed tomography-based radiomic prognostic marker of advanced high-grade serous ovarian cancer recurrence: A multicenter study. Front Oncol 2019;9.
[28] Yin P, Mao N, Zhao C, Wu J, Sun C, Chen L, et al. Comparison of radiomics machine-learning classifiers and feature selection for differentiation of sacral chordoma and sacral giant cell tumour based on 3D computed tomography features. Eur Radiol 2019;29:1841–7.
[29] Yin P, Mao N, Zhao C, Wu J, Chen L, Hong N. A Triple-classification radiomics model for the differentiation of primary chordoma, giant cell tumor, and metastatic tumor of sacrum based on T2-weighted and contrast-enhanced T1-weighted MRI. J Magn Reson Imaging 2019;49:752–9.
[30] Yin P, Mao N, Wang S, Sun C, Hong N. Clinical-radiomics nomograms for pre-operative differentiation of sacral chordoma and sacral giant cell tumor based on 3D computed tomography and multiparametric magnetic resonance imaging. Br J Radiol 2019;20190155.
[31] Wei W, Wang K, Tian K, Liu Z, Wang L, Zhang J, et al. A Novel MRI-based radiomics model for predicting recurrence in chordoma. Conf Proc IEEE Eng Med Biol Soc 2018;2018:139–42.
[32] Li L, Wang K, Ma X, Liu Z, Wang S, Du J, et al. Radiomic analysis of multiparametric magnetic resonance imaging for differentiating skull base chordoma and chondrosarcoma. Eur J Radiol 2019;118:81–7.
[33] Moons KG, Altman DG, Reitsma JB, Ioannidis JP, Macaskill P, Steyerberg EW, et al. Transparent reporting of a multivariable prediction model for individual prognosis or diagnosis (TRIPOD): explanation and elaboration. Ann Intern Med 2015;162:W1–W73.
[34] Luo W, Phung D, Tran T, Gupta S, Rana S, Karmakar C, et al. Guidelines for developing and reporting machine learning predictive models in biomedical research: a multidisciplinary view. J Med Internet Res 2016;18:e323.
[35] Ma J, Tian K, Du J, Wu Z, Wang L, Zhang J. High expression of survivin independently correlates with tumor progression and mortality in patients with skull base chordomas. J Neurosurg 2019;1–10.
[36] Aerts HJWL, Velazquez ER, Leijenaar RTH, Parmar C, Grossmann P, Carvalho S, et al. Decoding tumour phenotype by noninvasive imaging using a quantitative radiomics approach. Nat Commun 2014;5:4006.
[37] Simon N, Friedman J, Hastie T, Tibshirani R. Regularization paths for Cox's proportional hazards model via coordinate descent. J Stat Softw 2011;39:1–13.
[38] Camp RL, Dolled-Filhart M, Rimm DL. X-Tile. Clin Cancer Res 2004;10:7252.
[39] Strobl C, Malley J, Tutz G. An introduction to recursive partitioning: rationale, application, and characteristics of classification and regression trees, bagging, and random forests. Psychol Methods 2009;14:323–48.

[40] Youden WJ. Index for rating diagnostic tests. Cancer 1950;3:32–5.
[41] Akaike H. New Look at Statistical-Model Identification. Ieee T Automat Contr. 1974;Ac19:716-23.
[42] Balachandran VP, Gonen M, Smith JJ, DeMatteo RP. Nomograms in oncology: more than meets the eye. Lancet Oncol 2015;16:E173–80.
[43] Heagerty PJ, Lumley T, Pepe MS. Time-dependent ROC curves for censored survival data and a diagnostic marker. Biometrics 2000;56:337–44.
[44] Sun X, Xu WC. Fast implementation of DeLong's algorithm for comparing the areas under correlated receiver operating characteristic curves. IEEE Signal Proc Let 2014;21:1389–93.
[45] Stallard N. Simple tests for the external validation of mortality prediction scores. Stat Med 2009;28:377–88.
[46] Kramer AA, Zimmerman JE. Assessing the calibration of mortality benchmarks in critical care: The Hosmer-Lemeshow test revisited. Crit Care Med 2007;35:2052–6.
[47] Gillies RJ, Kinahan PE, Hricak H. Radiomics: images are more than pictures, They Are Data. Radiology 2016;278:563–77.
[48] Jager D, Lechel A, Tharehalli U, Seeling C, Moller P, Barth TFE, et al. U-CH17P, -M and -S, a new cell culture system for tumor diversity and progression in chordoma. Int J Cancer 2018;142:1369–78.
[49] Whelan JS, Davis LE. Osteosarcoma, chondrosarcoma, and chordoma. J Clin Oncol 2018;36:188–93.
[50] Esteva A, Kuprel B, Novoa RA, Ko J, Swetter SM, Blau HM, et al. Dermatologist-level classification of skin cancer with deep neural networks. Nature 2017;542:115.
[51] Kermany DS, Goldbaum M, Cai WJ, Valentim CCS, Liang HY, Baxter SL, et al. Identifying medical diagnoses and treatable diseases by image-based deep learning. Cell 2018;172:1122-+.
[52] LeCun Y, Bengio Y, Hinton G. Deep learning. Nature 2015;521:436–44.
[53] An SJ, Liu WQ, Venkatesh S. Fast cross-validation algorithms for least squares support vector machine and kernel ridge regression. Pattern Recogn 2007;40:2154–62.
[54] Bakker SH, Jacobs WCH, Pondaag W, Gelderblom H, Nout RA, Dijkstra PDS, et al. Chordoma: a systematic review of the epidemiology and clinical prognostic factors predicting progression-free and overall survival. Eur Spine J 2018;27:3043–58.
[55] Almefty KK, Pravdenkova S, Sawyer JR, Al-Mefty O. Impact of cytogenetic abnormalities on the management of skull base chordomas Clinical article. J Neurosurg 2009;110:715–24.
[56] Chugh R, Tawbi H, Lucas DR, Biermann JS, Schuetze SM, Baker LH. Chordoma: The nonsarcoma primary bone tumor. Oncologist 2007;12:1344–50.
[57] Schulz-Ertner D, Karger CP, Feuerhake A, Nikoghosyan A, Combs SE, Jakel O, et al. Effectiveness of carbon ion radiotherapy in the treatment of skull-base chordomas. Int J Radiat Oncol 2007;68:449–57.
[58] Wang S, Zhou M, Liu ZY, Liu ZY, Gu DS, Zang YL, et al. Central focused convolutional neural networks: Developing a data-driven model for lung nodule segmentation. Med Image Anal 2017;40:172–83.